Optics Letters

Transmission of 2 × 56 Gb/s PAM-4 signal over 100 km SSMF using 18 GHz DMLs

Shiwei Zhou,[1] Xiang Li,[2] Lilin Yi,[3] Qi Yang,[2] and Songnian Fu[1,*]

[1]Wuhan National Laboratory for Optoelectronics, and School of Optics and Electronic Information, Huazhong University of Science and Technology, Wuhan 430074, China
[2]State Key Laboratory of Optical Communication Technologies and Networks, Wuhan Research Institute of Posts and Telecommunications, Wuhan 430074, China
[3]State Key Laboratory of Advanced Optical Communication Systems and Networks, Shanghai Jiao Tong University, Shanghai 200240, China
*Corresponding author: songnian@mail.hust.edu.cn

Received 26 January 2016; revised 3 March 2016; accepted 7 March 2016; posted 9 March 2016 (Doc. ID 258282); published 12 April 2016

We experimentally demonstrate C-band 2 × 56 Gb/s pulse-amplitude modulation (PAM)-4 signal transmission over 100 km standard single-mode fiber (SSMF) using 18 GHz direct-modulated lasers (DMLs) and direct detection, without inline optical amplifier. A delay interferometer (DI) at the transmitter side is used to extend the transmission reach from 40 to 100 km. A digital Volterra filter at the receiver side is used to mitigate the nonlinear distortions. We obtain an average bit error ratio (BER) of 1.5×10^{-3} for 2 × 56 Gb/s PAM-4 signal after 100 km SSMF transmission at the optimal input power, which is below the 7% forward error correction (FEC) threshold (3.8×10^{-3}).

OCIS codes: (060.0060) Fiber optics and optical communications; (060.4080) Modulation; (060.4510) Optical communications.

http://dx.doi.org/10.1364/OL.41.001805

The rapid traffic growth within data centers has propelled the necessity to deploy the ultrahigh capacity metro optical links in short and medium reaches. Point-to-point high-speed optical interconnects prefer parallel intensity modulation (IM)/direct-detection (DD) optical links to achieve the transmission rate of up to 100 Gb/s with the goal of high bit-rate and low cost [1]. Besides the traditional on-off keying (OOK) format, some advanced modulation formats such as pulse amplitude modulation (PAM) and discrete multi-tone (DMT) have gained worldwide interest due to better performance and higher spectra efficiency [2–10]. Generally, PAM-4 has advantages in terms of implementation complexity and power consumption, while DMT requires smaller bandwidth. Meanwhile, for the purpose of cost reduction, the possibility of high-speed direct modulation without the need for an additional external optical modulator is highly desired. At present, 10 GHz direct-modulated lasers (DML) are commonly used. J. Man has demonstrated a 4 × 25 Gbps PAM-4 signal transmission, while F. Li has demonstrated a 256.51 Gb/s four-channel wavelength division multiplexed (WDM) 16QAM-DMT transmission [11,12]. In our early work, we experimentally demonstrated 112 Gb/s (4 × 28 Gb/s) PAM-4 signal over 160 km SSMF using 10 GHz DMLs [13]. Combining the higher-level modulation format and the wider bandwidth optical components makes it possible to achieve parallel 100 Gb/s or beyond low-cost metro-connection. To further extend the transmission reach, we have to increase the input power, leading to severe transmission impairments arising from the fiber nonlinearity. Furthermore, to mitigate transmission impairments, various methods have been proposed to cope with this problem, such as feed-forward equalization (FFE) [6,8] and maximum likelihood sequence estimation (MLSE) [8,14]. In the optical communications, Xia and Rosenkranz first proposed the nonlinear electrical equalizer (NLEE) based on Volterra filter (VF) which is applied for IM/DD transmission as an extension of commonly used feed-forward equalizers (FFE) and decision feedback equalizers (DFE) [15]. Although the VF-based equalizer has already been applied to either a coherent transmission system or a DMT transmission system [2,16], it has never been utilized for the PAM-4 signal transmission. Currently, the maximum transmission distance of 56 Gb/s PAM-4 at 1550 nm is limited to 26.4 km SSMF when the MLSE is used [14]. In this Letter, based on our earlier work [13], we experimentally demonstrate 100 km SSMF transmission of 112 Gb/s (2 × 56 Gb/s) PAM-4 signal with the help of 18 GHz DMLs. At the transmitter side, C-band 18 GHz DMLs are loaded with 56 Gb/s PAM-4 signals. A delay interferometer (DI) is utilized to extend the transmission reach [17]. To mitigate the nonlinear distortions during the SSMF transmission, the VF-based equalizer is applied in the digital signal processing (DSP) flow at the receiver side. Our experimental results show that by considering DI and the first third-order kernels of the VF-based equalizer, the SSMF transmission distance can be significantly increased from less than 40 to 100 km. To the best of our knowledge, this is the first time that 2 × 56 Gb/s PAM-4 signals transmit over 100 km SSMF without the inline optical amplification.

For the DML-based IM/DD transmission operating at the C-band, transmission impairments mainly come from three parts: (1) limited bandwidth of the optoelectronic devices; (2) interaction between chirp and chromatic dispersion (CD); and (3) fiber nonlinearities [18]. The limited electrical

bandwidth can be enhanced by a pre-emphasis technique at the transmitter side. As a result, high frequency attenuation can be partially compensated. The optical signal-to-noise ratio (OSNR) is severely deteriorated due to the interaction between the CD and the chirp. Since the traditional optical filter can only deal with single channel, we set the wavelength of DMLs periodically according to the free spectra range (FSR) of DI to improve the OSNR of all channels simultaneously. As for the CD, we realize the vestigial sideband modulation (VSB) to prevent the CD induced power fading [19]. Meanwhile, we can restrict the signal spectrum broaden by the frequency chirp, improve extinction ratio by filtering out the low frequency components, and convert the useless frequency modulation to the useful amplitude modulation [20,21]. It has been shown that the square-law detection for the IM/DD system introduces the undesired nonlinear noise, leading to the severe transmission performance degradation [22]. On the other hand, the fiber nonlinearity due to the high input power is another severe impairment. To solve the nonlinear problems after the SSMF transmission, we apply the VF-based equalizer to mitigate the nonlinear distortions. The k-th sample of the output signal after the digital equalizer can be described as [2]

$$\begin{aligned} y(k) = &\sum_{l_1=1}^{L_1-1} h_1(l_1)x(k-l_1) + \sum_{l_1=0}^{L_2-1}\sum_{l_2=0}^{l_1} h_2(l_1,l_2)\prod_{m=1}^{2} x(k-l_m) \\ &+ \sum_{l_1=0}^{L_3-1}\sum_{l_2=0}^{l_1}\sum_{l_3=0}^{l_2} h_3(l_1,l_2,l_3)\prod_{m=1}^{3} x(k-l_m) + \cdots \\ &+ \sum_{l_1=0}^{L_i-1}\sum_{l_2=0}^{l_1}\cdots\sum_{l_i=0}^{l_{i-1}} h_i(l_1,l_2,\cdots,l_i)\prod_{m=1}^{i} x(k-l_m) + \cdots, \end{aligned} \quad (1)$$

where $x(k-l_m)$ is the $(k-l_m)$-th sample of the received signal; $h_1(l_1)$, $h_2(l_1,l_2)$, $h_3(l_1,l_2,l_3)$, and $h_i(l_1,l_2,\cdots,l_i)$ are the 1st, 2nd, 3rd, and i-th order Volterra kernels; and L_1, L_2, L_3, and L_i are parameters of the VF-based equalizer, which defines the number of involved samples. Although applying higher-order term can be more accurate to model the nonlinearity, the computation complexity rapidly grows. As an illustration, the tap numbers of the first three kernels of the equalizer are L_1, $L_2(L_2+1)/2$, and $L_3(L_3+1)(L_3+2)/6$, respectively. To achieve a trade-off between the computation complexity and accuracy, it has been shown that up to third-order kernels are enough to describe the fiber optical transmission system [23], which is also verified by our experiment. As shown in Eq. (1), the first-order term represents traditional linear equalizer. The second-order term is induced by the square-law detection, and the third-order term is induced by the fiber nonlinearity representing the nonlinearity mitigation. Thus, in our following experiment, we will choose at most third-order kernels, which means that the total tap number is $L_1 + L_2(L_2+1)/2 + L_3(L_3+1)(L_3+2)/6$. To update these kernels, the adaptive filter algorithms such as least mean square (LMS) and recursive least square (RLS) can be selected. To obtain the optimal kernels, we use a decision-feedback algorithm to update the kernels by training symbols. Then we use the optimal kernels with the feed-forward algorithm to mitigate those distortions.

The schematic experimental setup is shown in Fig. 1. A pseudo-random bit sequence (PRBS) with a word length of $2^{23}-1$ is used for bit-to-symbol mapping and generation of the PAM-4 signal. The generated electrical PAM-4 signal is stored in a four-channel arbitrary waveform generator (Agilent Technologies, M8195A) with a sampling rate of 65 GSa/s. Instead of utilizing electrical microwave amplifier, the outputs of AWG directly modulate the two DMLs. Two 18 GHz DMLs are operated at 1549.81 and 1550.86 nm, respectively. The output signals from two DMLs are combined by an optical coupler (OC). An erbium-doped fiber amplifier (EDFA) is employed to control the input power. The FSR of DI is 66 GHz, which is half the channel spacing of two DMLs. Due to the limited choice of PD modules, a PD with a bandwidth of 40 GHz is used, which is not integrated with a transimpedance amplifier (TIA). Thus, we have to set another EDFA at the receiver side, which will introduce additional noise. It is noted that both distance extension and cost reduction can be achieved by removing the EDFA at the receiver side and choosing the proper PD module with TIA. To characterize the two channels, we use a OBPF to filter each channel individually. After the optical-to-electronic conversion, the electrical signals are sampled by a real-time oscilloscope (Tektronix DPO73304D) operating at 100 GSa/s and processed offline. The optical spectra of two DMLs are shown in Fig. 2(a), which are characterized by an optical spectrum analyzer (OSA) with the resolution of 0.01 nm. The joint frequency responses of both DML and PD at the wavelength of 1549.81 nm are shown in Fig. 2(b). The 3 and 10 dB electrical bandwidth at the back-to-back case are 14 and 20 GHz, respectively. As shown in Fig. 2(b), the severe power fading induced by the interaction between chirp and CD is observed after 80 km SSMF transmission without DI. When we detune the peak wavelength of DI to the shorter wavelength, the DI filters out the redshift chirp simultaneously, as shown in Fig. 2(a). In such a case, the notches due to the power fading vanish, as shown in Fig. 2(b). To investigate the effects of nonlinear distortions, we consider the digital equalizer in four cases: (1) with only the first kernel, which represents the traditional linear equalizer; (2) with the first and second kernels; (3) with the first and third kernels; and (4) with the first, second, and third kernels. After optimizing the equalizer parameters, we set the involved

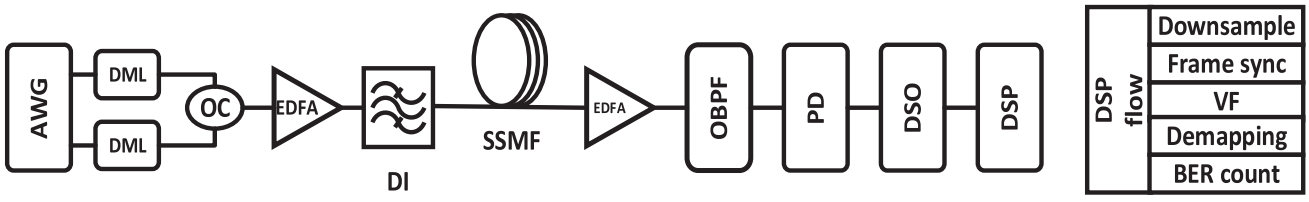

Fig. 1. Experimental setup. (AWG, arbitrary waveform generator; PD, photodetector; DSO, digital storage oscilloscope; DSP, digital signal processing).

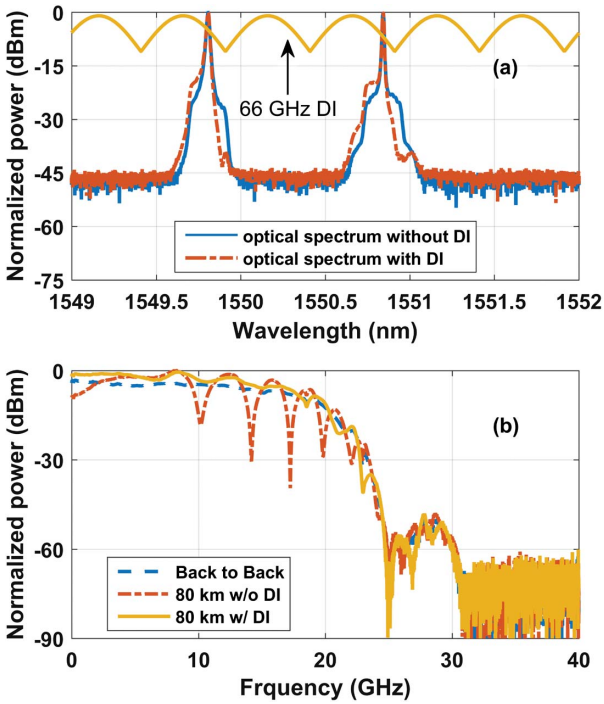

Fig. 2. Characteristics of the PAM4 signal. (a) Optical spectra with and without the DI. (b) Frequency response after the 80 km SSMF transmission.

samples L_1, L_2, and L_3 as 51, 17, and 13, which are defined as (51, 17, 13). In the following experiment, we will use these parameters, unless specifically mentioned.

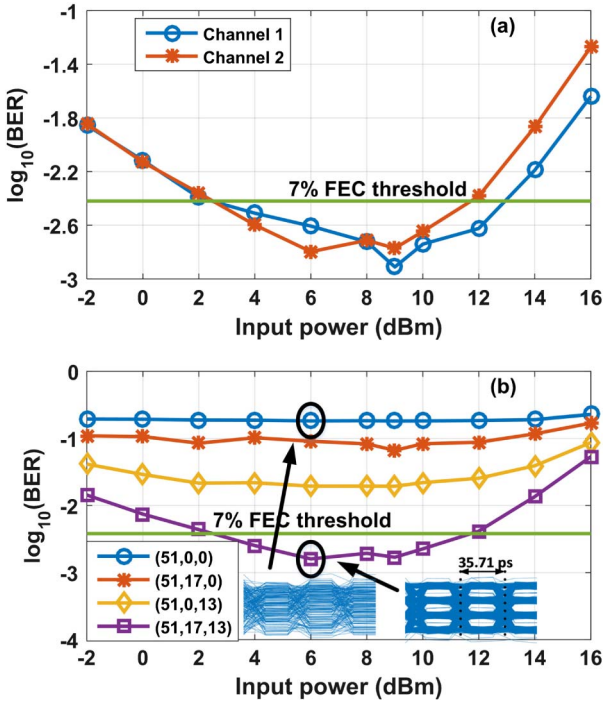

Fig. 3. BER performances of the 28 GBaud PAM4 signal versus the input power after the 100 km SSMF transmission. (a) Two channels. (b) Optimization of the digital equalizer. (Inset, 28 GBaud PAM-4 signal eye diagram).

Figure 3(a) shows the BER performances of two channels versus the input power after 100 km SSMF transmission. The received optical power before the optical-to-electronic conversion is 3 dBm. The power before the EDFA at the receiver side is not constant, which varies depending on the input power. Thus, we optimize the input power before the signal is launched to the 100 km SSMF, which is about 6 dBm. Figure 3(b) shows the BER performances of channel 2 at 1549.81 nm at the optimal input power for the equalizer with different order of kernels. As shown in Fig. 3(b), the performance is degraded if only using the lower-order kernel of the equalizer. We can also see that the VF-based equalizer with only first- and third-order kernels performs better than that with only first- and second-order kernels, which means that the third-order nonlinearity is more severe than the second-order nonlinearity after 100 km SSMF transmission. We further study the effects of a DI and VF-based equalizer with different parameters. As shown in Fig. 4(a), under the 7% FEC threshold, the use of DI can increase the transmission distance from less than 40 to 100 km. The reason for such improvement can be seen in Fig. 2, where the power fading in the frequency domain disappears with the help of DI. Figure 4(b) shows the performances of different parameters of the equalizer. As shown in Fig. 4(b), the BER performance is improved with the growing involved samples, indicating that the involved sample parameters of the equalizer can be optimized according to the SSMF transmission distance to achieve 7% FEC threshold. The equalizer with parameters of (21, 9, 5) and (41, 15, 5) is sufficient for the 60 and 80 km SSMF transmission, corresponding to the total tap number of only 101 and 196, respectively.

Furthermore, we experimentally investigate the transmission performance in terms of the computation efficiency and complexity after parameters optimization by considering both

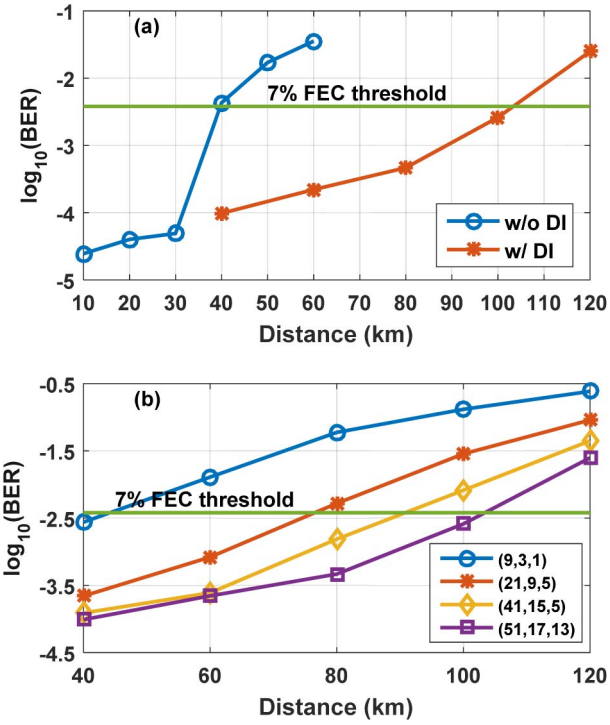

Fig. 4. BER performances of the 28 GBaud PAM4 signal versus the transmission distance for channel 2. (a) Effect of the DI. (b) Optimization of the digital equalizer.

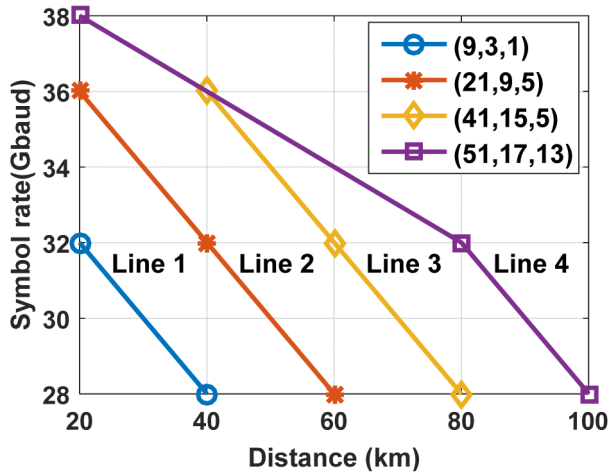

Fig. 5. BER performances versus the product of symbol-rate and transmission distance under the 7% FEC threshold for a different equalizer length.

transmission distance and symbol-rate. We define the efficiency as iterative times for searching the optimal kernels. We also define the complexity as the number of multiplications in a VF-based equalizer, namely $L_1 + 2 \times L_2(L_2 + 1)/2 + 3 \times L_3(L_3 + 1)(L_3 + 2)/6$. As we mentioned earlier, although both LMS and RLS can be used to update the kernels, the convergence speed is dramatically different. Although the selection of various parameters and SSMF transmission distance has little effect on its convergence speed, the convergence speed of RLS is much faster than that of the LMS. In our experiment, the stable state can be achieved after about 1,000 iterations by using the RLS. However, it requires more than 10,000 iterations for the LMS. To obtain an acceptable computational complexity for the different transmission scenario, different equalizer parameters are applied to recover the received signal to satisfy the 7% FEC threshold requirement. As shown in Fig. 5, it is obvious that with the decrement of either transmission distance or symbol-rate, the equalizer parameters can be reduced, indicating smaller computation complexity. The parameters of (51,17,13), (41,15,5), (21,9,5), and (9,3,1) require 1722, 386, 216, and 24 multiplications, respectively. The line in Fig. 5 indicates the upper bound of the combination of the transmission distance and symbol-rate for a specific parameters of the equalizer. From Line 1 to Line 3, the computation complexity grows slowly with the increase of distance and symbol-rate. However, the computation complexity grows fast in Line 4 with further increase of distance and symbol-rate. Thus, the VF-based digital equalizer is verified to be a useful tool to extend the SSMF transmission distance with the slowly growing computation complexity between the Line 1 and Line 3 areas. If we want to further improve the transmission performance, due to the limited electrical bandwidth, we have to face the problem of computation complexity.

In conclusion, we have experimentally demonstrated C-band 2 × 56 Gb/s PAM-4 signal transmission over 100 km SSMF based on 18 GHz DML. The DI is applied at the transmitter side to mitigate the power fading in the frequency domain induced by the interaction between the chirp and CD, while the nonlinear distortions are substantially mitigated by the digital VF-based equalizer. The DML-based two-channel PAM-4 transmission, with the help of both a DI and a VF-based equalizer, is shown as a good candidate for future low-cost optical metro-interconnection.

Funding. 863 High Technology Plan (2015AA015502); National Natural Science Foundation of China (NSFC) (61275069, 61331010, 61322507); State Key Laboratory of Optical Communication Technologies and Networks, Wuhan Research Institute of Posts & Telecommunications Open Fund (2016OCTN-01).

REFERENCES

1. H. Y. Chen, C.-C. Wei, C.-Y. Lin, L.-W. Chen, I. C. Lu, and J. Chen, *Proc. Optical Fiber Communication Conference (OFC)* (2015), paper Th1H.2.
2. C. Hsing-Yu, W. Chia-Chien, C. Hsuan-Hao, C. Yu-Chao, I. C. Lu, and C. Jyehong, *Proc. European Conference on Optical Communication (ECOC)* (2014), paper 3.21.
3. W. Yan, L. Li, B. Liu, H. Chen, Z. Tao, T. Tanaka, T. Takahara, J. Rasmussen, and D. Tomislav, *Proc. Optical Fiber Communication Conference (OFC)* (2014), paper M2I.4.
4. P. Dong, J. Lee, Y.-K. Chen, L. L. Buhl, S. Chandrasekhar, J. H. Sinsky, and K. Kim, *Proc. Optical Fiber Communication Conference (OFC)* (2015), paper Th5B.4.
5. L. Zhang, E. Zhou, Q. Zhang, X. Xu, G. N. Liu, and T. Zuo, *Proc. Optical Fiber Communication Conference (OFC)* (2015), paper Th4A.2.
6. H. Zhang, S. Fu, J. Man, W. Chen, X. Song, and L. Zeng, *Proc. Optical Fiber Communication Conference (OFC)* (2014), paper M2I.3.
7. B. Teipen, N. Eiselt, A. Dochhan, H. Griesser, M. Eiselt, and J. P. Elbers, *Proc. International Conference on Transparent Optical Networks (ICTON)* (2015), paper Mo.D3.3.
8. F. Karinou, C. Prodaniuc, N. Stojanovic, M. Ortsiefer, A. Daly, R. Hohenleitner, B. Kögel, and C. Neumeyr, IEEE Photonics Technol. Lett. **27**, 1872 (2015).
9. F. Karinou, R. Rodes, K. Prince, I. Roudas, and I. T. Monroy, *Proc. Optical Fiber Communication Conference/National Fiber Optic Engineers Conference* (2013), paper OW4A.2.
10. J. L. Wei, J. D. Ingham, D. G. Cunningham, R. V. Penty, and I. H. White, J. Lightwave Technol. **30**, 3273 (2012).
11. J. Man, W. Chen, X. Song, and L. Zeng, *Proc. Optical Fiber Communication Conference (OFC)* (2014), paper M2E.7.
12. F. Li, X. Xiao, J. Yu, J. Zhang, and X. Li, *Proc. European Conference on Optical Communication (ECOC)* (2015), paper Mo.4.5.5.
13. X. Li, S. Zhou, H. Ji, M. Luo, Q. Yang, L. Yi, R. Hu, C. Li, S. Fu, A. Alphones, W.-D. Zhong, and C. Yu, *Proc. Optical Fiber Communication Conference (OFC)* (2016), paper W1A.5.
14. C. Chen, X. Tang, and Z. Zhang, *Proc. Optical Fiber Communication Conference (OFC)* (2015), paper Th4A.5.
15. C. Xia and W. Rosenkranz, J. Lightwave Technol. **25**, 996 (2007).
16. R. Okabe, B. Liu, M. Nishihara, T. Tanaka, T. Takahara, L. Li, Z. Tao, and J. C. Rasmussen, *Proc. European Conference on Optical Communication (ECOC)* (2015), paper P. 5.18.
17. M. Bi, S. Xiao, H. He, L. Yi, Z. Li, J. Li, X. Yang, and W. Hu, Opt. Express **21**, 16528 (2013).
18. D. Sadot, G. Dorman, A. Gorshtein, E. Sonkin, and O. Vidal, Opt. Express **23**, 991 (2015).
19. W. A. Ling and I. Lyubomirsky, Opt. Express **22**, 6984 (2014).
20. J. Yu, Z. Jia, M. F. Huang, M. Haris, P. N. Ji, T. Wang, and G. K. Chang, J. Lightwave Technol. **27**, 253 (2009).
21. L. S. Yan, Y. Wang, B. Zhang, C. Yu, J. McGeehan, L. Paraschis, and A. E. Willner, Opt. Express **13**, 5106 (2005).
22. C. Ju, X. Chen, and Z. Zhang, *Proc. Optical Fiber Communication Conference (OFC)* (2014), paper Tu2G.6.
23. K. V. Peddanarappagari and M. Brandt-Pearce, J. Lightwave Technol. **15**, 2232 (1997).